Kinetics of Phase Separation by Spinodal Decomposition in Mixtures of Telechelic Hydroxy-Terminated Polyisobutylene and Poly(tetrahydrofuran)

Hak-soo Lee,† Thein Kyu,*,† Avi Gadkari,‡,§ and Joseph P. Kennedy‡

Institutes of Polymer Engineering and Polymer Science, The University of Akron, Akron, Ohio 44325

Received January 25, 1991; Revised Manuscript Received April 19, 1991

ABSTRACT: Time-resolved light scattering has been employed to study the phase separation kinetics of hydroxy-terminated polyisobutylene (HO-PIB-OH)/poly(tetrahydrofuran) (HO-PTHF-OH) mixtures. A coexistence curve was constructed by conventional cloud-point measurement. The system reveals an upper critical solution temperature (UCST) with a maximum at 75 wt % HO-PTHF-OH at 43 °C, and it is reversible. Several temperature quench experiments with the 75 wt % HO-PTHF-OH mixture were carried out from a single-phase region (52 °C) to a two-phase region (38, 36, 34, and 32 °C). Dissolution studies were undertaken from 30 °C to a single-phase region at 45, 47, 49, and 51 °C. The spinodal temperature was 42 °C for the 75 wt % HO-PTHF-OH mixture. The time evolution of scattering profiles was analyzed by the linearized Cahn–Hilliard theory for the initial stage of spinodal decomposition (SD) and by dynamic scaling laws for the late growth regime of SD. The possibility of perturbing phase separation by the onset of crystallization of HO-PTHF-OH is discussed.

Introduction

Networks, particularly those of well-defined structures, are of considerable interest for both academic and industrial researchers.[1,2] Two-component mixed networks are a unique class of networks i.e., networks comprising two chemically different kinds of randomly connected chains, for example, a polar/nonpolar chain system or a hydrophilic/hydrophobic combination.

Two-component polar/nonpolar networks have recently been prepared by randomly connecting well-defined hydroxy telechelic polyisobutylene (HO-PIB-OH) and hydroxy telechelic poly(tetrahydrofuran) (HO-PTHF-OH) prepolymers with stoichiometric quantities of diisocyanate.[3] These two-component mixed networks were found to be biocompatible upon in vivo implantation for 11 weeks in rats.[3] Similarly, networks comprising a hydrophilic and a hydrophobic component, so-called amphiphilic networks, are also biocompatible and of great potential interest for biomaterial applications, e.g., biomembranes and soft-tissue replacement.[4,5]

In the course of these investigations, we became interested in the exploration of the fundamentals of polymer/polymer miscibility of polar/nonpolar network constituents. This paper concerns the phase separation behavior of HO-PIB-OH/HO-PTHF-OH mixtures and the effect of HO-PTHF-OH crystallization on the process involved.

Experimental Section

The HO-PTHF-OH used (Du Pont Co.) was $\bar{M}_n = 2000$. Hydroxy-terminated HO-PIB-OH was prepared by living cationic polymerization,[6-8] and it had $\bar{M}_n = 1500$ and $\bar{M}_w/\bar{M}_n = 1.06$. The prepolymers were mixed manually at ~70 °C for 10 min, and then a small amount of the mixtures was placed on oval slide glasses. Bubbles trapped during mixing were removed in a vacuum oven (~70 °C, 1 Torr, 10 min) until the specimens became clear and bubble-free. The samples were carefully covered with thin slide glasses and cooled to room temperature.

* To whom correspondence should be addressed.
† Institute of Polymer Engineering.
‡ Institute of Polymer Science.
§ Present address: Exxon Chemical Company, Baytown Polymer Research Center, Baytown, TX 77520.

The cloud-point phase diagram was obtained by light scattering; the procedure is described elsewhere.[9] The setup included a He–Ne laser light source operating at 632.8 nm. The scattered intensity was detected by a two-dimensional Vidicon camera interfaced with an optical multichannel analyzer (OMA III, Model 1460, EG&G Princeton Applied Research Co.). Thermal dependencies of cloud points were checked by varying the heating and cooling rates. The equilibrium cloud point versus composition was established by extrapolating to a zero heating rate.

Temperature quench experiments were performed from a single-phase region (52 °C) to a two-phase region (32–38 °C). To follow the dynamics of phase decomposition, several temperature jumps were carried out from 30 °C to a single-phase region (45–51 °C).

Results and Discussion

Phase Diagram. Cloud-point measurements of mixtures were carried out at various heating/cooling rates of 1, 0.5, and 0.1 °C/min. The data were extrapolated to a zero heating rate to obtain the coexistence curves. As shown in Figure 1, the HO-PIB-OH/HO-PTHF-OH system exhibits the characteristics of an upper critical solution temperature (UCST) with a maximum at ~75 wt % HO-PTHF-OH at 43 °C. A reversible phase change is observed as expected for low molecular weight polymer mixtures.[10,11] When a binary liquid mixture phase separates by SD, a highly interconnected regular structure develops. In light-scattering studies, a scattering halo corresponding to the reciprocal of average periodic distances of phase-separated domains initially appears and persists during the early stage and then shifts to a smaller diameter due to domain growth. Figure 2 exhibits such a representative optical micrograph together with a scattering halo obtained upon quenching the liquid mixture of 75 wt % HO-PTHF-OH from a single-phase region (52 °C) to an unstable two-phase region (ambient temperature). These observations are common for a phase separation by SD.[12]

Early Stage of SD. Several T-quench experiments were carried out to elucidate the dynamics of SD in the 75 wt % HO-PTHF-OH mixture. Figure 3 exhibits the scattering profiles obtained following a T quench from 52 to 32 °C. The scattering maximum initially appears at a large wavenumber ($q \sim 6\ \mu m^{-1}$), and the peak position

0024-9297/91/2224-4852$02.50/0

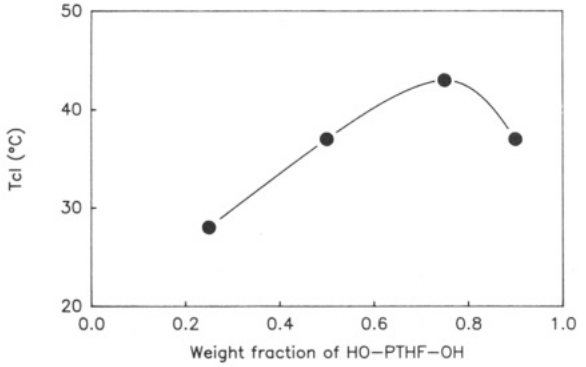

Figure 1. Equilibrium phase diagram for HO-PIB-OH/HO-PTHF-OH mixtures.

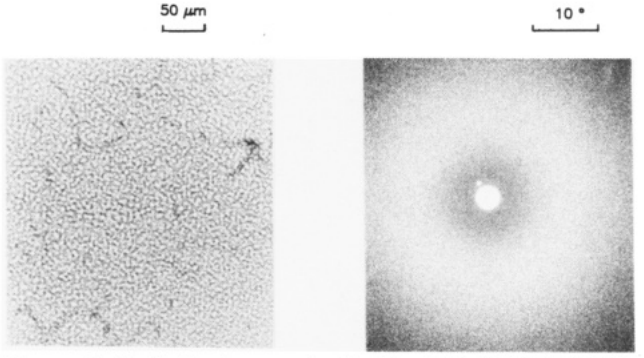

Figure 2. Optical micrograph of a 75 wt % HO-PTHF-OH mixture revealing interconnected domains and the corresponding scattering halo during spinodal decomposition.

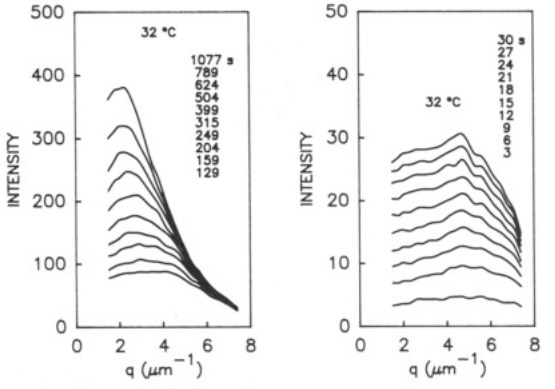

Figure 3. Time evolution of scattering peaks following a temperature quench from 52 to 32 °C.

remains virtually invariant for some time; it shows little or no movement. As time elapses, the peak moves toward smaller scattering angles due to domain growth. Peak invariance is one of the features predicted by the linearized theory originally developed by Cahn and Hilliard,[13,14] assuming a negative composition diffusivity (up-hill diffusion) based on the fluctuation dissipation theorem. The linearized theory predicts exponential growth for the scattering function; i.e.,

$$I(q,t) = I(q,t=0)\ \exp\{2R(q)t\} \tag{1}$$

where t is the phase separation time and q the scattering wavenumber defined by $q = (4\pi/\lambda)\sin(\theta/2)$. λ and θ are the wavelength of light and the scattering angle measured in the medium, respectively. $R(q)$ represents the growth rate of composition fluctuations of the mixture, which may be further expressed as

$$R(q) = -Mq^2\{\partial^2 f/\partial c^2 + 2\kappa q^2\} \tag{2}$$

where f is the local free-energy density, c the local concentration, κ the coefficient of composition gradient,

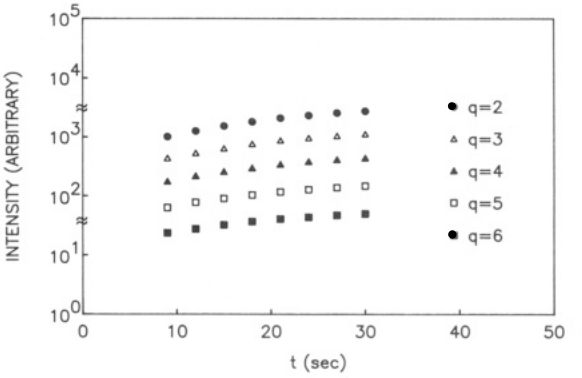

Figure 4. Logarithmic intensity vs time plots for 75 wt % HO-PTHF-OH mixtures at various scattering wavenumbers.

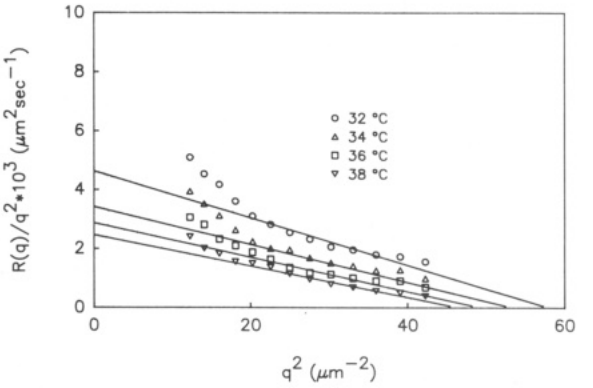

Figure 5. Cahn's plots of $R(q)/q^2$ vs q^2 for various temperature quenches.

and M the mobility. The deficiency of eq 1 was first pointed out by Cook,[15] who modified the linear theory by incorporating thermal fluctuations associated with clustering and short-range order of the stable single phase. The modified equation may be expressed as

$$S(q,t) = S_s(q) + [S_0(q) - S_s(q)]\ \exp\{2R(q)t\} \tag{3}$$

$$S_s(q) \sim I_s(q) \tag{4}$$

where $S_0(q)$ is proportional to the scattered intensity at $t = 0$ and $S_s(q)$ is the virtual structure factor, i.e., an extrapolated structure function from a two-phase region to a single-phase region, assuming continuity of the system.[16,17] Therefore, the measured intensity needs to be corrected for parasitic scattering, dark current, and thermal fluctuations. These contributions were combined into background scattering, which can be measured for a single phase. The true intensity can be obtained by subtracting the background scattering from the observed intensity. The semilogarithmic plot of scattered intensity vs time gives an exponential increase for a limited period, and then it deviates from the linear slope (Figure 4). $R(q)$ values were calculated from the slopes and replotted in Figure 5 in accordance with eq 2, i.e., $R(q)/q^2$ vs q^2. Except for a few points at low q, the data may be approximated by linear slopes with the aid of the following equation

$$q_m^2 = {}^1/_2 q_c^2 \tag{5}$$

where q_c is a crossover wavenumber and q_m is the peak wavenumber. At low q, these data are somewhat affected by residual parasitic scattering. The deviation at high q may be caused by the onset of crystallization of HO-PTHF-OH, particularly at deep quenches.

The applicability of the linearized theory to polymeric mixtures has been investigated by various groups.[18-24]

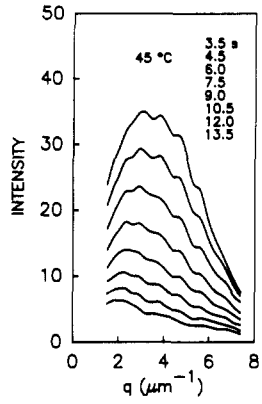

Figure 6. Time decay of scattering profiles of the 75 wt % HO-PTHF-OH mixture following a T jump from 30 to 45 °C.

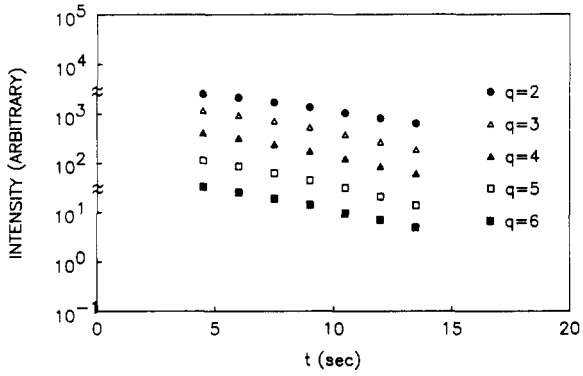

Figure 7. Logarithmic intensity vs time plots for the 75 wt % HO-PTHF-OH mixture during phase dissolution.

Hashimoto and co-workers[18,19] observed an appreciable period where the linearized theory is operative. Han and Okada[20] also confirmed the applicability of the linearized theory during the early stage of SD for polystyrene/poly(vinyl methyl ether) blends. A similar conclusion was also reached for a linear regime of polycarbonate/poly(methyl methacrylate) mixtures.[21]

Phase Dissolution. The T-jump experiments were carried out from 30 to 45–51 °C. As shown in Figure 6, the scattered intensity decays rapidly while showing a slight movement of the peak position to a smaller angle. In order to obtain the true intensity, the final equilibrium intensity was subtracted from the measured intensity. The time-lag for equilibrating the mixtures at a given temperature is 3–5 s and was subtracted from the total experiment time. A similar observation was made by Osamura et al.,[24] who reported the increase of periodic particle distance during phase dissolution in Al–Zn alloys; i.e., the scattering angle showed a movement to lower scattering angles. They estimated the time lag to be about 2 s, which is consistent with our observation. The authors concluded that during the phase dissolution the average particle sizes increase at the expense of the faster decay of the smaller fluctuations.

The decay of scattered intensity was plotted as a function of phase dissolution time on a semilogarithmic scale (Figure 7). The data are fairly linear for most wavenumbers, suggesting exponential decay of the scattered intensity. The decay rates $-R(q)$ were plotted against q^2 in Figure 8. The data can be fitted reasonably well with linear slopes from which the apparent diffusivities may be determined as demonstrated by Kumaki and Hashimoto[25] for polystyrene/poly(vinyl methyl ether) blends. The apparent diffusivities were evaluated by Fick's law; i.e., $R(q) = -D_{app}q^2$. The temperature dependence of the apparent diffusivities during dissolution was plotted in Figure 9

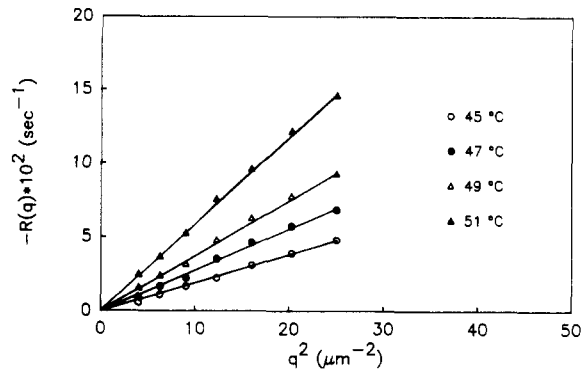

Figure 8. q^2 dependence of decay rate $R(q)$ of the 75 wt % HO-PTHF-OH mixture.

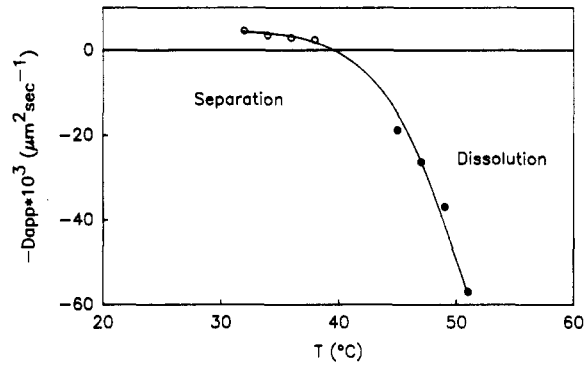

Figure 9. Temperature dependence of apparent diffusivities for various T quenches and T jumps of the 75 wt % HO-PTHF-OH mixture.

together with that of the phase separation. The solid line was drawn by using nonlinear regression. The temperature at which the diffusivity becomes zero is regarded as the spinodal point (T_s). T_s is estimated to be 42 °C for the 75 wt % HO-PTHF-OH system. Near T_s, the diffusivity may be scaled as

$$D_{app} = D_0\epsilon^{\nu} \tag{6}$$

with

$$\epsilon = (T - T_s)/T_s \tag{7}$$

where D_0 is the self-diffusion coefficient and ν is the critical exponent, which was measured to be 0.66 for a number of low molecular weight solutions.[26,27] Nojima et al.[28] obtained ν values of around 0.75 for polystyrene/poly(methylphenylsiloxane) oligomer mixtures. In spite of the big differences between the experimental and spinodal temperature, the present system shows $\nu = 0.8 \pm 0.1$ in Figure 10, a value that is between those for monomeric solutions and polymer blends and is consistent with the observation of Nojima et al.[28]

Late Stage of SD. As discussed in the preceding sections, SD in the HO-PIB-OH/HO-PTHF-OH mixture follows the linearized theory for a short period and then starts to obey the power law, i.e.,

$$q_m(t) = t^{-\varphi} \tag{8}$$

and

$$I_m(t) = t^{\psi} \tag{9}$$

where the subscript m stands for the maximum values. The exponents φ and ψ are predicted by various authors.[29-34] Langer, Baron, and Miller (LBM),[29] based on the nonlinear scheme, computed $\varphi = 1/6$ for the early regime and $\varphi = 0.21$ for the later coarsening. Binder and Stauffer,[30] based on the cluster reaction, predicted $\varphi =$

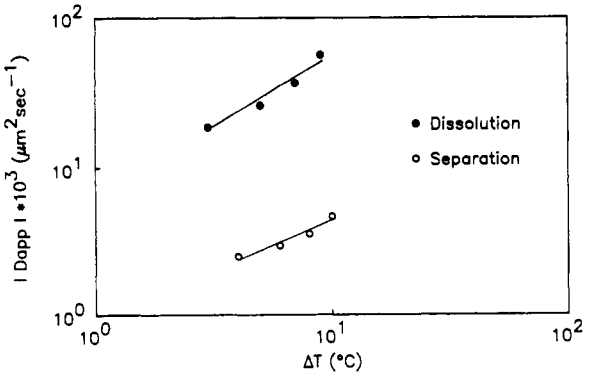

Figure 10. log–log plot of apparent diffusivities as a function of ΔT ($=T - T_s$) for phase separation and dissolution for 75 wt % HO-PTHF-OH.

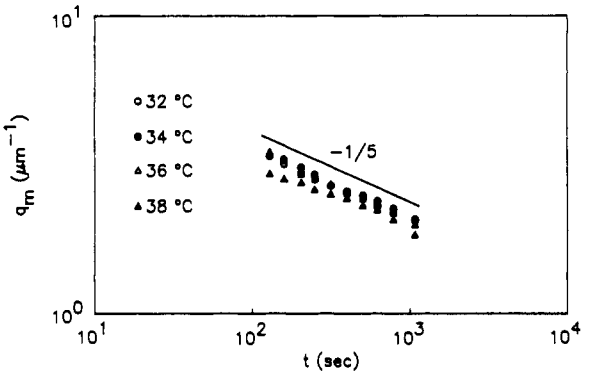

Figure 11. log–log plot of maximum wavenumber vs phase separation time.

$1/(3 + d)$ for the low-temperature regime, with d being the dimensionality of growth. Later, Binder[31] obtained $\varphi = 1/(2 + d)$ for an intermediate regime after a complicated initial stage and $\psi = 3\varphi$ for these temperatures at late stages with $\varphi = {}^1/_3$ and $\psi = 1$. With the percolation approach by taking into consideration the influence of hydrodynamic interactions on the coarsening rate and combining through diffusive coalescence, Siggia[32] obtained the same equation but with $\varphi = {}^1/_3$ for the early growth regime and $\varphi = 1$ for the intermediate to late stages (flow stage) caused by surface tension.

Figure 11 exhibits log–log plots of the peak wavenumber vs phase separation time. φ was estimated to be ${}^1/_5$, which is in good agreement with LBM's and Binder's prediction for an intermediate regime, $\varphi = 1/(2 + d)$ with $d = 3$ for three-dimensional growth. As discussed below, the incorporation of a crystalline component seems to retard domain growth; thus, growth could not reach the cluster dynamic regime ($\varphi = {}^1/_3$) during the time scale of the experiment.

Since the scattering peak wavenumber (q_m) appears to be constant for an appreciable period, the correlation length (ξ) in the single phase may be considered as the initial fluctuation size of SD at $t = 0$

$$\xi = 1/q_m(t=0) \tag{10}$$

The universal curve may then be established with dimensionless variables Q_m and τ, which may be scaled as

$$Q_m = q\xi \tag{11}$$

and

$$\tau = D\xi^{-2}t \tag{12}$$

where D and ξ were already obtained from the early stage analyses. As shown in Figure 12, the universal curves superpose quite well. A slope of $-{}^1/_5$ is obtained, which is

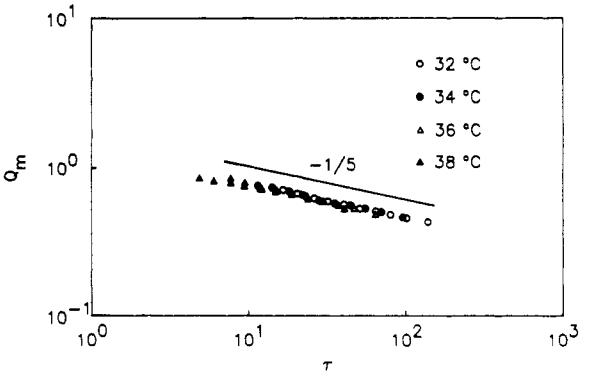

Figure 12. Universal master curve with dimensionless variables Q_m vs τ.

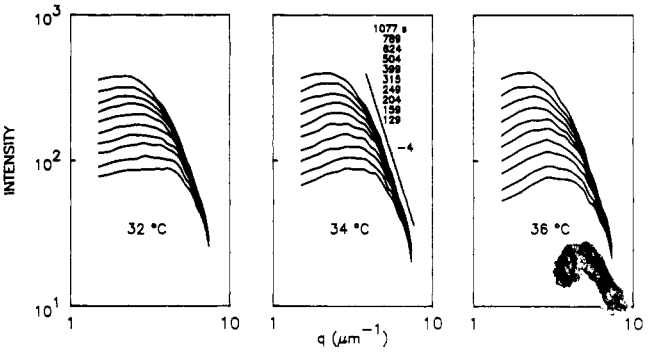

Figure 13. Plot of $I(q)q_m^3$ vs q/q_m for a self-similarity test.

appreciably lower than that obtained in a previous case for epoxy/rubber mixtures,[35] where the crossover from $-{}^1/_6$ to $-{}^1/_3$ was seen. This exponent coincidentally corresponds to the prediction of the LBM theory for the intermediate stage of SD. However, the mechanism may be different as the interplay of the crystallizing component with phase separation may decelerate domain growth; thus, growth does not reach the cluster regime where the coalescence of cluster domains takes place within the time scale of the experiment.

Self-Similarity. At very late stages of growth, geometrical shapes of growing domains show self-similar behavior.[36] A relationship exists between the scattered intensity, $I(q,t)$, and the scaled structure function, $s(x)$, at a given time, t

$$I(q,t) \sim V\langle\eta^2\rangle\xi(t)^3 s(x) \tag{13}$$

with

$$x = q\xi(t) \tag{14}$$

where V is the irradiated volume and $\langle\eta^2\rangle$ the mean square concentration fluctuation. Here, $\xi(t)$ in turn relates to the wavelength of periodic structure $\Lambda(t)$ by the following equation:

$$\xi(t) = \Lambda(t)/2\pi = 1/q_m(t) \tag{15}$$

From eqs 13 and 15, the structure function can be described as

$$s(x) \sim I(q,t)q_m^3(t) \tag{16}$$

In the early stage of SD, $\langle\eta^2(t)\rangle$ varies quite rapidly; therefore, the structure function cannot be scaled by a single correlation length, $\xi(t)$. We therefore employed the data of the late stages of SD for this scaling test. As shown in Figure 13, the $s(x)$ vs x plot shows an acceptable superposition for different phase separation times, suggesting that self-similarity may be attained as the structure function exhibits temporal universality. It appears that

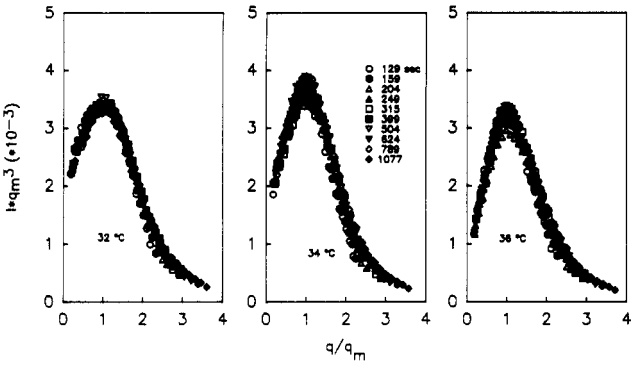

Figure 14. log–log plot of scattering function vs scattering wavenumber for various times.

phase separation may be fully developed; otherwise, master curves could not be obtained, suggesting a late stage of SD rather than an intermediate stage. This fact in turn suggests that the exponent of $-1/5$ may not correspond to the intermediate stage, as predicted by the LBM theory. Hence, it may be concluded that phase separation may be affected by the onset of crystallization of HO-PTHF-OH, particularly at deep quenches, thereby giving lower slopes (q_m vs t and Q_m vs τ).

A scaled structure function was proposed by Furukawa as follows:

$$S(x) = \frac{(1 + \gamma/2)x^2}{\gamma/2 + x^{2+\gamma}} \tag{17}$$

where $x = q/q_m$. $S(x) \sim x^2$ for $x < 1$ and $S(x) \sim x^{-\gamma}$ for $x \gg 1$. For the critical composition, $\gamma = 2d$, and for off-critical composition, $\gamma = d + 1$ with d being the dimensionality of growth. The shape of the scattered intensity is predicted as $I \sim q^2$ at $q < q_m$ and $I \sim q^{-\gamma}$ at $q > q_m$. For three-dimensional growth, $\gamma = 6$ for the critical composition and $\gamma = 4$ for off-critical mixtures. Figure 14 shows log–log plots of intensity vs wavenumber for the 75 wt % HO-PTHF-OH mixture. The value of γ is ~ 4, which suggests that the SD of the 75 wt % HO-PTHF-OH system is similar to the behavior of off-critical mixtures. This finding also suggests that the maximum composition in the cloud-point phase diagram does not necessarily guarantee that it is the critical mixture. The slopes of 2 and 4 have been reported for metal alloys,[37] oligomer mixtures,[38] and polymer solutions.[28] In the case of critical mixtures of polystyrene and poly(vinyl methyl ether), Hashimoto et al.[39] obtained the values of 2 and 6, respectively. Recently we also observed the slopes of 2 and 6 for the critical mixture of polycarbonate/poly(methyl methacrylate).[40] The slope of -4 is generally regarded as Porod's law[41] in the analysis of small-angle X-ray scattering. The good agreement with Porod's law suggests that the boundaries of phase-separated domains are sharp and smooth at least in the length scale of the wavelength of light. Thus, the possibility of surface fractal may be ruled out.

Conclusions

Phase separation occurs by SD in HO-PIB-OH/HO-PTHF-OH mixtures. The approximation of the early stage of SD by the linearized Cahn–Hilliard theory is fairly good. According to the kinetic studies, the spinodal temperature is 42 °C. The kinetic exponent shows an exponent of $-1/5$ for late stages of phase growth. Such a low exponent may be due to the onset of crystallization of HO-PTHF-OH, which may retard the phase growth, although it coincidentally agrees with the prediction of the LBM theory. The behavior of the universal curve of the HO-PIB-OH/HO-PTHF-OH mixture and those of mixtures of solutions, oligomers, and some polymer blends is very similar. Self-similarity is observed in the regime where the structure function shows universality with time. The phase separation dynamics of the 75 wt % HO-PTHF-OH mixture shows behavior predicted for an off-critical mixture with slopes of 2 and -4. The -4 slope is in good accord with Porod's law, thereby suggesting that the phase boundaries of this mixture are sharp and smooth in the scale length of the wavenumber of light.

Acknowledgment. Support by the members of the Polymer Engineering Research Communication (PERC) and partial support from the National Science Foundation, Grant 89-20826, are gratefully acknowledged.

References and Notes

(1) Mark, J. E. *Adv. Polym. Sci.* **1982**, *44*, 1.
(2) Miyabayashi, T.; Kennedy, J. P. *J. Appl. Polym. Sci.* **1986**, *31*, 2523.
(3) Gadkari, A.; Kennedy, J. P.; Kory, M. M.; Elby, D. L. *Polym. Bull.* **1989**, *22*, 25.
(4) Chen, D.; Kennedy, J. P.; Kory, M. M.; Elby, D. L. *J. Biomed. Mat. Res.* **1989**, *23*, 1327.
(5) Kennedy, J. P. U.S. Patent 4,942,204, 1990.
(6) Ivan, B.; Kennedy, J. P.; Chang, V. S. C. *J. Polym. Sci., Polym. Chem. Ed.* **1980**, *18*, 3177.
(7) Faust, R.; Kennedy, J. P. *J. Polym. Sci., Part A, Polym. Chem.* **1987**, *25*, 1847.
(8) Faust, R.; Nagy, A.; Kennedy, J. P. *J. Macromol. Sci., Chem.* **1987**, A24 (6), 595.
(9) Kyu, T.; Saldanha, J. M. *J. Polym. Sci., Polym. Lett. Ed.* **1988**, *26*, 33.
(10) Nojima, S.; Nose, T. *Polym. J.* **1982**, *14*, 269.
(11) Russell, T. P.; Hadziionnou, G.; Warburton, W. K. *Macromolecules* **1985**, *18*, 78.
(12) Synder, H. L.; Meakin, P.; Reich, S. *Macromolecules* **1983**, *16*, 757.
(13) Cahn, J. W. *J. Chem. Phys.* **1965**, *42*, 93.; *Trans Metall. Soc. AIME* **1968**, *242*, 1649.
(14) Hilliard, J. E. *Phase Transformations*; ASME: Fairfield, NJ, 1968; p 497.
(15) Cook, H. E. *Acta Metall.* **1970**, *18*, 297.
(16) Binder, K. *J. Chem. Phys.* **1983**, *79*, 6387.
(17) Sato, T.; Han, C. C. *J. Chem. Phys.* **1988**, *88*, 2057.
(18) Hashimoto, T.; Kumaki, J.; Kawai, H. *Macromolecules* **1983**, *16*, 641.
(19) Takenaka, M.; Izutami, T.; Hashimoto, T. *Macromolecules* **1987**, *20* 2257.
(20) Okada, M.; Han, C. C. *J. Chem. Phys.* **1985**, *85*, 5317.
(21) Kyu, T.; Saldanha, J. M. *Macromolecules* **1988**, *21*, 1021.
(22) Bates, F. S. *Bull. Am. Phys. Soc.* **1989**, *34*, 653.
(23) Oono, Y.; Puri, S. *Phys. Rev. Lett.* **1987**, *58*, 836.
(24) Osamura, K.; Okuda, H.; Amemiya, Y.; Hashizume, H. In *Dynamics of Ordering Processes in Condensed Matter*; Komura, S., Furukawa, H., Eds.; Plenum: New York, 1989; p 273.
(25) Kumaki, J.; Hashimoto, T. *Macromolecules* **1986**, *19*, 763.
(26) Kuwahara, N.; Fenly, D. V.; Tamsky, M.; Chu, B. *J. Chem. Phys.* **1970**, *55*, 1140.
(27) Chou, Y. C.; Goldburg, C. M. *Phys. Rev. A* **1981**, *24*, 3205.
(28) Nojima, S.; Ohyama, Y.; Yamaguchi, M.; Nose, T. *Polym. J.* **1982**, *14*, 907.
(29) Langer, J. S.; Baron, M.; Miller, H. S. *Phys. Rev. A* **1975**, *11*, 1417.
(30) Binder, K.; Stauffer, D. *Phys. Rev. Lett.* **1973**, *33*, 1006.
(31) Binder, K. *Phys. Rev. B* **1977**, *15*, 4425.
(32) Siggia, E. D. *Phys. Rev. A* **1979**, *20*, 595.
(33) Furukawa, H. *J. Appl. Crystallogr.* **1988**, *21*, 805.
(34) Snyder, H.; Meakin, P. *J. Chem. Phys.* **1986**, *85*, 6118.
(35) Lee, H. S.; Kyu, T. *Macromolecules* **1990**, *23*, 459.
(36) Furukawa, H. *Phys. Rev. Lett.* **1979**, *43*, 136.
(37) Komura, S.; Osamura, K.; Fujii, H.; Takeda, T. *Phys. Rev. B* **1984**, *30*, 2944.; **1985**, *31*, 1278.
(38) Takahashi, M.; Horiuchi, H.; Kinoshita, S.; Ohyama, Y.; Nose, T. *J. Phys. Soc. Jpn.* **1988**, *55*, 2689.
(39) Hashimoto, T.; Itakura, M.; Hasegawa, H. *J. Chem. Phys.* **1986**, *85*, 6118.
(40) Lim, D. S.; Kyu, T. *J. Chem. Phys.* **1990**, *92*, 3951.
(41) Porod, G. *Kolloid Z.* **1951**, *124*, 83.